arXiv:cond-mat/0204137v2 [cond-mat.soft] 9 Jun 2002

Creation of a molecular condensate by dynamically melting a Mott-insulator

D. Jaksch,[1] V. Venturi,[3] J.I. Cirac,[2] C.J. Williams,[3] and P. Zoller[1]
[1] *Institute for Theoretical Physics, University of Innsbruck, A–6020 Innsbruck, Austria.*
[2] *Max-Planck Institut für Quantenoptik, Hans-Kopfermann Str. 1, D-85748 Garching, Germany. and*
[3] *Atomic Physics Division, National Institute of Standards and Technology, Gaithersburg, Maryland 20899-8423.*

We propose creation of a molecular Bose-Einstein condensate (BEC) by loading an atomic BEC into an optical lattice and driving it into a Mott insulator (MI) with exactly two atoms per site. Molecules in a MI state are then created under well defined conditions by photoassociation with essentially unit efficiency. Finally, the MI is melted and a superfluid state of the molecules is created. We study the dynamics of this process and photoassociation of tightly trapped atoms.

PACS numbers: 03.75.Fi, 42.50.-p, 42.50.Ct

The generation of Bose Einstein condensates (BEC) of dilute atomic gases has resulted in a remarkable series of experiments demonstrating various properties of quantum degenerate gases [1]. One of the next major goals in this effort is the realization of a molecular BEC. A promising route towards a molecular condensate is the conversion of an atomic BEC to molecules via photoassociation, a process discussed so far for conditions of quasi-homogeneous trapping of atomic gases [2, 3, 4, 5]. In this Letter we describe a novel path to create condensates of composite atomic objects, in particular a molecular BEC, based on photoassociation via a *Mott insulator state* of bosonic atoms trapped in an optical lattice [6, 7]. This provides an efficient way of generating a molecular BEC, avoiding some of the problems encountered in the quasi-homogeneous case [2]. It also touches upon fundamental questions related to the formation of a BEC by "melting" of a Mott-insulator (MI) state in a quantum phase transition, as opposed to the familiar growth from a thermal cloud of atoms [8].

Experimental advances in manipulating BECs [1], and in particular the loading of a BEC into an optical lattice generated by interfering laser beams have recently led to a seminal experiment by I. Bloch and collaborators [7]. They demonstrated a quantum phase transition from a BEC or superfluid (SF) state into a MI by varying the lattice laser intensity, as proposed theoretically in [6]. While a SF phase has long range order, the MI phase corresponds to the loading of a precise number of atoms into each lattice site, i.e. Fock state occupation of lattice sites. Among the proposed applications of this new atomic quantum phase are the study of ultracold controlled collisions and quantum computing with neutral atoms [9]. In the present context, the MI phase opens the possibility to efficiently create a molecular BEC in the following four steps: (i) an atomic BEC is loaded into an optical lattice, (ii) the depth V_0 of the optical lattice is increased to create a MI with *exactly two particles per lattice site*, (iii) a molecular MI state is produced by two-color photoassociation of the atoms under tight trapping conditions, and (iv) by decreasing the depth of the optical lattice the MI state is "melted", and thus a molecular BEC is created in a quantum phase transition.

At the end of step (i) above, we have an ensemble of bosonic atoms illuminated by orthogonal, standing wave laser fields tuned far from atomic resonance. These laser fields generate a potential for atomic motion of the form $V(\vec{x}) = \sum_{i=1}^{3} V_{0i}\sin^2(kx_i)$ with $k = 2\pi/\lambda$ the wavevector of the light and lattice period $a = \lambda/2$. The dynamics of bosonic atoms occupying the lowest Bloch band of an optical lattice is well described by the Bose-Hubbard model (BHM) [6] which includes the interaction U_a between particles occupying the same lattice site and the tunneling J_a of particles from one site to the next. The BHM Hamiltonian is given by

$$H_a = -J_a \sum_{\langle i,j\rangle} a_i^\dagger a_j + \sum_i \epsilon_i \hat{n}_i + \frac{1}{2} U_a \sum_i \hat{n}_i(\hat{n}_i - 1) \quad (1)$$

where a_i is a bosonic destruction operator of a particle at site i. The number of particles in site i is given by the operator $\hat{n}_i = a_i^\dagger a_i$, and ϵ_i is an energy offset due to an external trapping potential. The first sum in Eq. (1) runs over all nearest neighbors denoted by $\langle i, j\rangle$. Increasing the laser intensity of the trapping laser tends to compress atoms near the nodes of the lattice field, and thus leads to an increased on-site interaction U_a, while the atomic tunneling rate J_a decreases [6]. The BHM predicts a quantum phase transition from the SF phase to the MI state: according to mean field theory this occurs at the critical value $U_a^{(c)} \approx 5.8 z J_a$ [10] with z the number of nearest neighbors of each site. This corresponds to a (moderate) potential depth of $V_0 = 10E_R$ where $E_R = \hbar^2 k^2/2m$ is the recoil energy for atoms with mass m.

We will first illustrate the dynamics of the BHM Hamiltonian with a time dependent depth $V_0(t)$ of the optical lattice controlled by the laser intensity, leading to a variation $U_a(t)$ and $J_a(t)$ in Eq. 1. We assume the system initially to be in the SF ground state and calculate its time evolution for the time dependence shown in Fig. 1a [6]. For a model problem of N particles, where N is small (≈ 10), in a few lattice sites, the time dependent Schrödinger equation for the wave function $\Psi(t)$ can be solved exactly. Fig. 1b plots the eigenval-

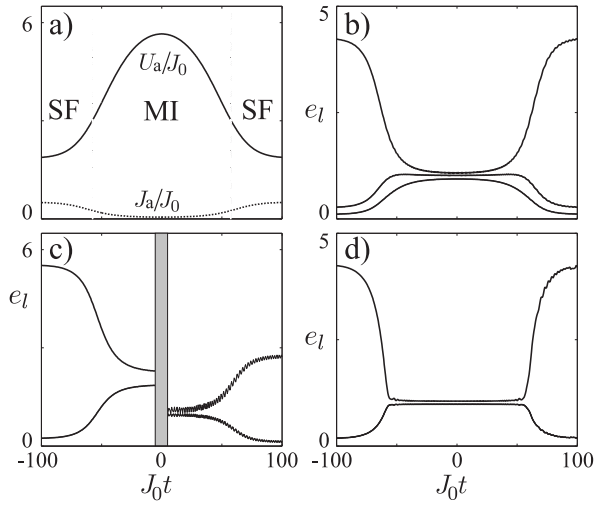

FIG. 1: a) Time dependence of U_a (solid curve) and J_a (dotted curve). The vertical dashed lines separate the SF and MI regions expected for adiabatic time evolution of the system in 1D. Parameters: we assume ^{87}Rb and $\lambda = 390$nm with $V_0(t) = V_{\rm SF} + (V_{\rm MI} - V_{\rm SF})/(1+\exp((t^2 - t_w^2)/t_s^2))$, $t_w = 30/J_0$, $t_s = 40/J_0$, $V_{\rm MI} = 20E_R$, $V_{\rm SF} = 5E_R$ giving $J_0 = 0.13E_R$. J_0/z is the hopping matrix element for $t \to -\infty$ b) Transition from the SF to the MI back to the SF phase for atoms. We plot e_l (lower two curves are doubly degenerate) against t for $N = M = 5$ in a 1D lattice with periodic boundary conditions. c) Atoms in the SF phase are driven to a MI phase (time interval $t < 0$), converted to a molecular MI phase by a Raman pulse (shaded region around $t = 0$), and melted to obtain a molecular BEC ($t > 0$). We plot e_l (lower curve doubly degenerate) for the atoms (molecules) before (after) the conversion for $N/2 = M = 3$ in 1D, and parameters $J_b = J_a/2$, $U_a = U_b = U_{ab}$ with time dependence given in Fig. 1a). d) Same as b) but using the Gutzwiller ansatz (the lower curve is four fold degenerate).

ues e_l of the one particle density matrix $\rho_{i,j} = \langle a_i^\dagger a_j \rangle$ ($\equiv \langle \Psi(t)|a_i^\dagger a_j|\Psi(t)\rangle$). As expected, there is one large eigenvalue for $U_a < U_a^{(c)}$ of the order of the number of particles. The corresponding wave function is approximately given by $|\psi_{\rm SF}\rangle \propto (\sum_i a_i^\dagger)^N |{\rm vac}\rangle$ for N particles in M sites with $|{\rm vac}\rangle$ the vacuum state. All the other eigenvalues are small and are associated with the quantum depletion of the SF state. As U_a increases and crosses the critical point $U_a^{(c)}$ all eigenvalues tend towards one, corresponding to a diagonal single particle density operator (MI). Upon ramping U_a down again the SF is restored.

An extension of the BHM (1) in an optical lattice describes the situation with atoms and molecules present. Denoting the annihilation operator of a molecule by b_i, we add to the Hamiltonian (1) a tunneling J_b and on-site interaction term U_b for molecules, and an atom-molecule interaction term of the form $H_{a-b} = U_{ab} \sum_i b_i^\dagger b_i a_i^\dagger a_i$. The underlying assumption is that the laser beams generate an optical lattice for atoms and molecules with the same structure of nodes and antinodes, although both lattices can have different depth. The process of atom-molecule conversion by photoassociation is described by the Hamiltonian $H_{\rm conv} = \Omega(t) \sum_i \left(b_i^\dagger a_i a_i + {\rm h.c.} \right)/\sqrt{2}$, where $\Omega(t)$ is an effective Rabi frequency which is turned on at time $t = 0$ for a short time interval to convert two atoms at one lattice site into one molecule. In practice, this process will consist of several Raman steps to go to the molecular ground state (see Fig. (2)).

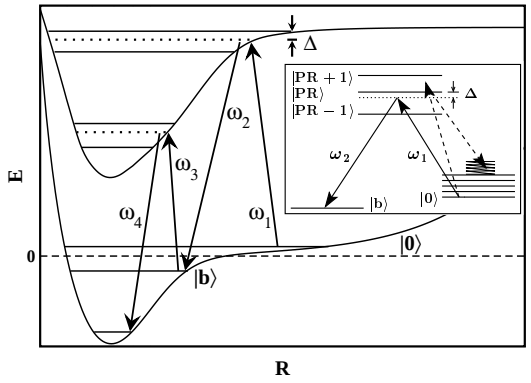

FIG. 2: Production of ground state molecules using two Raman transitions. The inset shows the first Raman transition (solid lines) and the process where ω_2 is absorbed before ω_1 (dashed lines). For ^{87}Rb and for a trap frequency of $\nu =$ 1MHz, $E_0 \approx 2$ MHz and outer turning point $R_{TP} \approx 500\, a_0$ (a_0=0.0529nm). For the singlet pathway, $E_b \approx -32$ GHz and $R_{TP} \approx 32\, a_0$.

We emphasize several distinguishing key features of the atom-molecule conversion process in an optical lattice. First conversion is most efficient under tight trapping conditions (in a regime where tunneling between lattice sites is negligible). The high atomic densities associated with the strong compression of the atoms opens inelastic collision channels that typically quench all lattice sites with three or more atoms. Thus we assume that only lattice sites with occupation of two (or one) atom survive the lattice compression. These loss processes are added to our Hubbard dynamics by writing down a master equation for a density matrix that includes these decay channels. However, since in the MI phase atomic number fluctuations are small, there are only a very few lattice sites that are actually depleted by this loss process. Second, for (exactly) two atoms trapped at one lattice site we have a complete microscopic understanding of the two-atom dynamics, and the conversion to molecules by photoassociation [11] beyond the effective description contained in the Hubbard model.

The two-atom Schrödinger equation [11] at a given lattice site separates for harmonic confinement into center-of-mass and relative coordinates. The potential curves for the relative motion of the two atoms in the trap are schematically shown in Fig. 2: for small distances

R we have the familiar molecular Born-Oppenheimer potentials while the large R-behavior is dominated by the trap confinement. The trapping potential discretizes the molecular continuum (scattering) states to form a series of harmonic oscillator trap states with frequency $\nu = (4V_0E_R)^{1/2}/\hbar$ with V_0 the potential depth. The goal is to perform a Rabi flop $\Omega T = \pi$ from the lowest trap state of two atoms (i.e. the state associated with the lowest atomic Bloch band) to a bound molecular state, with Ω the two-photon Rabi frequency. The discreteness of the trap states makes this a bound-bound Raman transition. The condition for not exciting any other trap states, i.e. to avoid heating, is $\Omega \ll \nu$. On the other hand, for incoherent processes (as spontaneous decay from the intermediate state) with effective decay rate γ to be small, we must have $\gamma T \ll 1$. Thus we require a large two-photon Rabi frequency and tight trapping, $\gamma \ll \Omega \ll \nu$. Note that Ω involves a matrix element from the bound trap state to a molecular state, which results in a scaling $\Omega \propto \nu^{3/4}$ [11], i.e. under conditions of tight trapping the two-photon Rabi frequency will be significantly enhanced. We will give specific numbers for these parameters for the case of ^{87}Rb below. Thus it is the preparation of the two-atom MI phase together with strong confinement which guarantees the coherent conversion of atoms to molecules with essentially unit efficiency.

Fig. 1c shows results from the exact integration of the Schrödinger equation for three sites with six atoms. Starting from the SF phase, the atoms are driven to the MI phase and converted into molecules at $t = 0$. Melting of the molecular MI phase then produces a molecular SF.

To describe the dynamics with a large number of particles in 2D and 3D we employ a time dependent mean field approximation based on a Gutzwiller ansatz [10]. For simplicity of writing we consider for the moment the case of atoms alone, where we write the wave function as the product of superposition states at the various lattice sites, $|G(t)\rangle = \prod_{i=1}^{M} \left(\sum_{n=0}^{\infty} f_n^{(i)}(t)|n\rangle_i \right)$. This ansatz is motivated by the success and simplicity of time-independent Gutzwiller mean field theory to model the ground state and phase diagram of the BHM [10]. The ground state is obtained from the variational principle $\langle G|H|G\rangle - \mu\langle G|\hat{N}|G\rangle \rightarrow \min$, where μ is a chemical potential introduced to enforce a given mean particle number [6]. From the time-dependent variational principle, $\langle G(t)|i\hbar\frac{\partial}{\partial t} - H(t)|G(t)\rangle \rightarrow \min$, the following time dependent equation is readily derived:

$$\begin{aligned} i\dot{f}_n^{(i)} &= \frac{U_a}{2} n(n-1) f_n^{(i)} \\ &\quad - J_a \sum_{\langle i,j \rangle} \left(\Phi_j^* f_{n+1}^{(i)} \sqrt{n+1} + \Phi_j f_{n-1}^{(i)} \sqrt{n} \right), \end{aligned} \tag{2}$$

where $\Phi_i \equiv \langle G|a_i|G\rangle = \sum_n f_{n-1}^{(i)*} \sqrt{n} f_n^{(i)}$ is the atomic SF density. Eq. (2) is a nonlinear equation for the amplitudes $f_l^{(i)}$, which preserves both normalization of the wave function and the mean particle number. In the SF limit and for a coherent state distribution of $f_n^{(i)} = \psi_i^n \exp(-|\psi_i|^2/2)/\sqrt{n!}$, Eq. (2) reduces to a time-dependent Gross-Pitaevskii equation for ψ_i on a lattice.

By projection to a state with definite particle number N, $|G_N\rangle = \mathcal{P}_N|G\rangle / \|\mathcal{P}_N|G\rangle\| \sim \int_0^{2\pi} d\varphi \exp(iN\varphi) \prod_{i=1}^{M} (\sum_{n=0}^{\infty} \exp(-in\varphi) f_n^{(i)} |n\rangle_i)$ a more consistent description is obtained. The resulting time dependent Schrödinger equation for the amplitudes $f_n^{(i)}$ is significantly more complex. It can be shown, however, that $f_n^{(i)}$ of the number projected Gutzwiller wave function again obey Eq. (2), provided the variance of the particle numbers at each lattice site satisfies $\Delta n_i \gg 1/\sqrt{N}$ (where $\Delta n_i^2 \equiv \langle n_i^2 \rangle - \langle n_i \rangle^2$ with $\langle n_i^2 \rangle = \sum_n n^2 |f_n^{(i)}|^2$ and $\langle n_i \rangle = \sum_n n |f_n^{(i)}|^2$). Note that this excludes the regime where we have a *precise* locking of the particle number, i.e., $f_n^{(i)} = \delta_{n,n_0}$, as in the MI obtained from the non-number conserving Gutzwiller for a homogeneous situation, when the number of particles N is commensurate with the lattice sites M and $n_0 = N/M$. However, a precise Fock state is never realized in the time evolution we consider since the initial superfluid density is not completely destroyed while ramping the optical lattice up. Also, an additional trap potential confining the system to a certain region in space ensures the existence of a remnant superfluid component. Below we model the evolution of an initial SF to an (approximate) MI while changing U_a and J_a by integrating mean field equations of the type (2). Fig. 1d gives the results obtained from Gutzwiller theory with initial state given by the time-independent Gutzwiller wave function, to be compared with the exact integration of the time dependent Schrödinger equation in 1D for a few particles in Fig. 1b. As expected, mean field theory shows a more pronounced phase transition than the few atom 1D calculation.

Using a generalization of the Gutzwiller ansatz to include superposition states of atoms and molecules, $|G(t)\rangle = \prod_{i=1}^{M} \left(\sum_{n_a,n_b=0}^{\infty} f_{n_a,n_b}^{(i)}(t)|n_a,n_b\rangle_i \right)$, where n_a and n_b refer to the atomic and molecular occupation, respectively, we have numerically investigated the creation of a molecular BEC in a 2D lattice with a superimposed harmonic trapping potential. The results are shown in Fig. 3. As expected we find that molecules are only created in sites with an atomic occupation of two before the Raman process (cf. Fig. 3b). They are surrounded by a ring of atoms which originates from those site with an atomic occupation of one before the Raman transition (see Fig. 3c). Finally, Fig. 3d shows the superfluid molecular density after ramping the optical lattice down.

We now turn to the description of the coherent Raman transitions involved in creating molecules in step (iii) of our scheme. There are several constraints on the choice of detunings and laser intensities (see Fig. 2) to maximize Ω. First, the detuning Δ from an allowed ex-

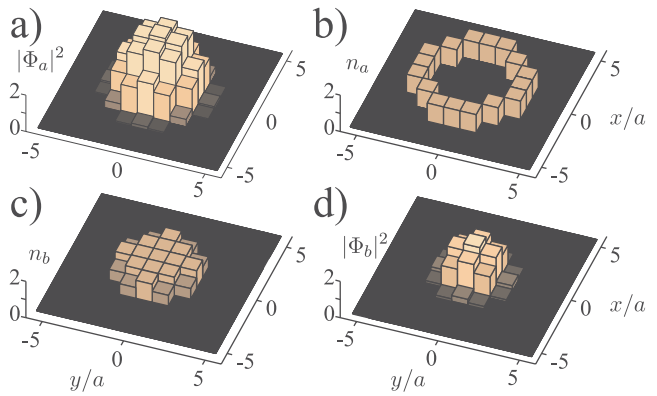

FIG. 3: 2D lattice. a) Initial atomic SF density $|\Phi_a|^2$. b) Number of atoms n_a and c) number of molecules n_b immediately after Raman conversion. d) Final SF molecular density $|\Phi_b|^2$. The chemical potential is $\mu = 2.5J_0$, the additional trap potential is given by $\epsilon_i = 2J_0(x_i^2 + y_i^2)/5a^2$, where x_i, y_i denote the coordinates of well i. The depth of the optical lattice is changed 10 times slower than in Fig. 1.

cited photoassociation resonance $|\Psi_{\rm PR}\rangle$ (cf. Fig. 2) must be large compared to the natural linewidth γ_{PR} of the intermediate state to suppress spontaneous Raman scattering. Also, one should not detune half-way between two resonances since interference between these two intermediate states will lead to a minimum in the effective two-photon Rabi frequency Ω. For appropriate choices of Δ and the intermediate state $|\Psi_{\rm PR}\rangle$, the coupling to all intermediate states other than $|\Psi_{\rm PR}\rangle$ can be neglected. Second, as outlined above, we have to ensure that the process where a ω_2 photon is absorbed before a ω_1 photon (schematically shown in the inset of Fig. 2) has negligible probability. This process causes trap excitations of single atoms and thus leads to heating. If both of these conditions are fulfilled the effective Rabi frequency Ω on Raman resonance for the first Raman step is given by $\Omega = \Omega_1\Omega_2/2\Delta$, where $\Omega_{1,2}$ are the Rabi frequencies for the first (second) step, and the effective spontaneous emission rate is $\gamma = \gamma_{\rm PR}\Omega_1^2/4\Delta^2$.

For the case of ^{87}Rb, the following Raman pathway is viable for producing $X^1\Sigma_g^+(v=0, J=0)$ molecules:

$$X^1\Sigma_g^+(v_{\rm trap}=0) \rightarrow A^1\Sigma_u(v=213) \rightarrow X^1\Sigma_g^+(v=120)$$
$$X^1\Sigma_g^+(v=120) \rightarrow A^1\Sigma_u(v=185) \rightarrow X^1\Sigma_g^+(v=52)$$
$$X^1\Sigma_g^1(v=52) \rightarrow A^1\Sigma_u(v=24) \rightarrow X^1\Sigma_g^+(v=0). \quad (3)$$

A two-step Raman pathway also exists for producing $a^3\Sigma_u^+(v=0, J=0)$ molecules. For the first step of the singlet pathway, the vibrational spacing near the $A^1\Sigma_u(v=213)$ level is 110 GHz, $\gamma_{PR} \approx 12$ MHz, and the binding energy of the $X^1\Sigma_g^+(v=120)$ is 31.9 GHz. Given a trap frequency ν of 1 MHz and intensities $I_1 = 1{\rm W/cm}^2$ and $I_2 = 10^{-3}{\rm W/cm}^2$ for the first Raman step of Eq. (3), one obtains $\Omega_1 = 0.71$ MHz and $\Omega_2 = 3.7$ MHz. For a red detuning of 200 linewidths we get $\Omega = 1.1$ kHz and and an effective spontaneous Raman scattering rate of $\gamma = 5.5$ Hz. For the process described in the preceding paragraph one finds that the undesirable $\omega_2 - \omega_1$ process has a blue detuning of 29.5 GHz off the same intermediate level and a Rabi frequency that is more than a factor of 100 below Ω. Although the pathway for producing singlet molecules is partially optimized, no attempt to optimize the intensities and detunings has been made. However we have chosen values to show that the undesirable $\omega_2 - \omega_1$ process can be sufficiently suppressed. The rate limiting step in the overall pathway is determined by the matrix element of the first Raman step. The matrix elements for all subsequent steps are at least 3-orders of magnitude larger than this one.

For experimental purposes, molecules in higher lying vibrational levels of the $X^1\Sigma_g^+$ or $a^3\Sigma_u^+$ state should also allow the formation and detection of a molecular BEC. Vibrational relaxation caused by inelastic molecule-molecule collisions, that ultimately limits the lifetime of the resulting molecular condensate, will in general be strongly suppressed as the kinetic energy in the exit channels increases. This occurs as the vibrational spacing increases and should allow for observations of molecular BEC for moderately bound vibrational levels.

In conclusion, generation of a MI phase of atoms allows efficient conversion of atoms to molecules, and to obtain a molecular condensate via "melting" in a quantum phase transition. This idea can be immediately generalized to e.g. heteronuclear molecules, or one could use laser chemistry to build more complex composite objects (trimers etc.) and, possibly, corresponding condensates by quantum melting. The key to designing these processes is the fact that the MI phase provides us with a given small number of particles per lattice site (reaction partners) whose few body dynamics can be understood in all detail and controlled via laser interactions.

Discussions with E. Tiesinga, P.S. Julienne and R. Grimm are gratefully acknowledged. Work supported in part by the Austrian Science Foundation, EU Networks, and by the U.S. Office of Naval Research.

[1] J.R. Anglin and W. Ketterle, Nature, **416**, 211 (2002).
[2] R. Wynar *et al.*, Science **287**, 1016 (2000); P. D. Drummond *et al.*, cond-mat/0110578; K. Goral, M. Gajda, and K. Rzazewski, Phys. Rev. Lett. **86**, 1397 (2001).
[3] M. Mackie, R. Kowalski, and J. Javanainen, Phys. Rev. Lett. **84**, 3803 (2000); J. Javanainen and M. Mackie, Phys. Rev. Lett. **88**, 90403 (2002).
[4] M. Holland, J. Park, and R. Walser, Phys. Rev. Lett. **86**, 1915 (2001).
[5] C. Gabbanini *et al.*, Phys. Rev. Lett. **84**, 2814 (2000),
[6] D. Jaksch, *et al.*, Phys. Rev. Lett. **81**, 3108 (1998).
[7] M. Greiner, *et al.*, Nature **415**, 39 (2002).
[8] H.-J. Miesner et al., Science 279, 10051007 (1998).

[9] For a review see: T. Calarco, *et al.* Fortschritte der Physik, **48**, 945 (2000).
[10] M.P.A. Fisher *et al.*, Phys. Rev. B **40**, 546 (1989); K. Sheshadri *et al.*, Europhys. Lett. **22**, 257 (1993); J.K. Freericks and H. Monien, Europhys. Lett. **26**, 545 (1994); L. Amico and V. Penna, Phys. Rev. Lett. **80**, 2189 (1998).
[11] F. H. Mies, E. Tiesinga, and P. S. Julienne, Phys. Rev. A **61**, 022721 (2000).